

Parallel Medical Imaging: A New Data-Knowledge-Driven Evolutionary Framework for Medical Image Analysis

Chao Gou, *Member, IEEE*, Tianyu Shen, Wenbo Zheng, Oliver Kwan, and Fei-Yue Wang, *Fellow, IEEE*

Abstract—There has been much progress in data-driven artificial intelligence technology for medical image analysis in last decades. However, it still remains a challenge due to its distinctive complexity of acquiring and annotating image data, extracting medical domain knowledge, and explaining the diagnostic decision for medical image analysis. In this paper, we propose a data-knowledge-driven evolutionary framework termed as Parallel Medical Imaging (PMI) for medical image analysis based on the methodology of interactive ACP-based parallel intelligence. In the PMI framework, computational experiments with predictive learning in a data-driven way are conducted to extract medical knowledge for diagnostic decision support. Artificial imaging systems are introduced to select and prescriptively generate medical image data in a knowledge-driven way to utilize medical domain knowledge. Through the parallel evolutionary optimization, our proposed PMI framework can boost the generalization ability and alleviate the limitation of medical interpretation for diagnostic decision. A GANs-based PMI framework for case studies of mammogram analysis is demonstrated in this work.

Index Terms—Parallel Intelligence, Evolutionary Optimization, Parallel Medical Imaging.

I. INTRODUCTION

MEDICAL image analysis aims at extracting clinically useful information from computed tomography (CT), positron emission tomography (PET), magnetic resonance (MR), ultrasound, X-ray and other modalities of images with the assistance of computers for diagnostic decision support [1], [2]. With urgent requirements of medical imaging, medical societies have entered a new era that medical equipments, image data, domain knowledge, and humans including physicians and patients are coupled in the large scale cyber-physical-social spaces (CPSS). Hence, vision-based medical image analysis is becoming an increasingly prominent role at many clinical workflow stages from screening and diagnosis to treatment delivery, especially in the domain of remote medical

consultation. Recently, vision-based medical image analysis have achieved promising results for skin cancer diagnosis [3], [4], red lesion detection in fundus images [5], mammography analysis [6], [7] and pulmonary nodule detection [8]. However, there are still challenges for vision-based medical image analysis. Firstly, these data-driven techniques require large scale of effective medical images annotated by domain experts or radiologists. Secondly, conventional methods for medical imaging are built in a data-to-knowledge way where algorithms are learned from existing training samples in a bottom-up manner without any feedback or interaction to utilize the medical domain knowledge. Last but not the least, there is a limitation in interpretability for final medical diagnostic decision made by learned ‘black-box’ models especially for the non-linear deep neural networks.

ACP methodology was first proposed in [9] for modeling, managing and controlling the complex systems, and it consists of *Artificial societies*, *Computational experiments* and *Parallel execution*. The ACP-based parallel intelligence is one form of intelligence generated from the interactions and executions between physical and artificial systems [10]. As part of parallel intelligence, parallel learning framework is presented in [11] to address issues of data collection and policy exploring in current machine learning framework. Parallel learning combines descriptive learning, predictive learning, and prescriptive learning into a uniform evolutionary framework to optimize the learning system by self-boosting [12].

Inspired by the interactive ACP-based parallel intelligence, we propose a data-knowledge-driven framework termed as Parallel Medical Imaging (PMI) to address the aforementioned challenges in medical image analysis. The proposed overall framework of PMI is illustrated in Fig.1. Firstly, as pointed by Wang *et al.* in [13] that evaluations of the objectives can be performed only based on data collected from physical world and virtual world, we propose to conduct computational experiments to predictively extract medical knowledge for diagnostic decision support that are explainable to humans in a data-driven way. Different from conventional medical image analysis frameworks that solely perform data-to-knowledge extraction, we further introduce artificial imaging systems to select and generate specific medical image data for data collection in a knowledge-driven way. Specifically, interactive parallel learning with descriptive and prescriptive scheme based on the explainable knowledge is performed to achieve knowledge-to-data generation in top-down manner that allows for boosting the performance of decision model. In addition,

This work was supported in part by the National Natural Science Foundation of China under Grant 61806198, 61533019 and Project of Youth Foundation of the State Key Laboratory for Management and Control of Complex Systems under Grant Y6S9011F4N.

C. Gou, T. Shen, and F.-Y. Wang are with the State Key Laboratory for Management and Control of Complex Systems, Institute of Automation, Chinese Academy of Sciences, Beijing 100190, China, Qingdao Academy of Intelligent Industries, Qingdao 266109, China, T. Shen is also with University of Chinese Academy of Sciences, Beijing 100049, China, and F.-Y. Wang is also with the Institute of Systems Engineering, Macau University of Science and Technology, Macau 999078, China. (e-mail: gouchao2012@ia.ac.cn, shen-tianyu2016@ia.ac.cn, feiyue.wang@ia.ac.cn) W. Zheng is with School of Software Engineering, Xi'an Jiaotong University, Xi'an 710049, China (e-mail: zwb2017@stu.xjtu.edu.cn). O. Kwan is with New Wheel Capital, Shanghai 201204, China. (e-mail: Okwan@newwheelcap.com)

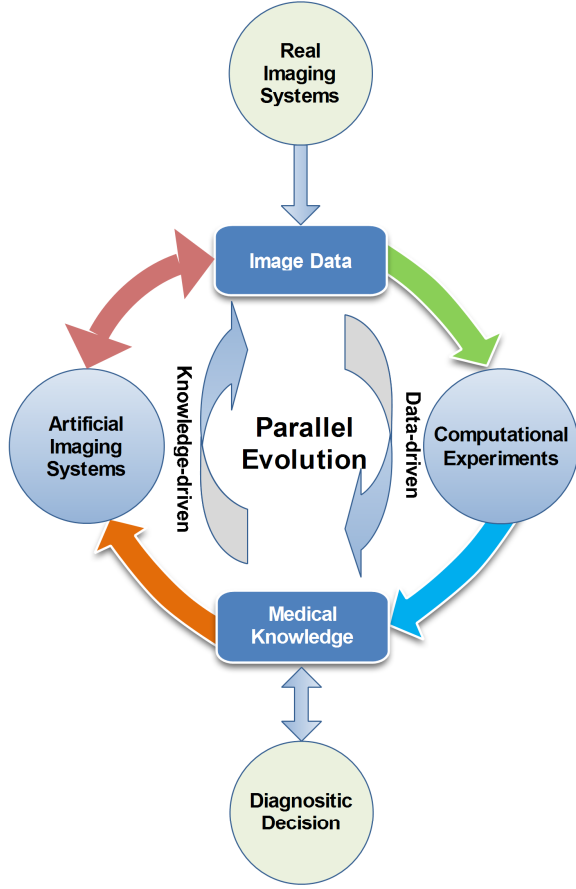


Fig. 1. Proposed Parallel Medical Imaging: A Data-Knowledge-Driven Framework.

the data-knowledge-driven parallel evolution can enable effective large scale data collection and enhance the interpretability of diagnosis.

The rest of this paper is arranged as follows. The preliminary of ACP-based parallel intelligence is presented in Section II. More details are given about our proposed Parallel Medical Imaging (PMI) framework in Section III. In Section IV, a case study about mammography with a implementation of PMI based on generative adversarial networks (GANs) is presented. Current challenges and insights are discussed in Section V. Conclusions are drawn in Section VI.

II. PRELIMINARY

A. ACP methodology

The ACP methodology was initially proposed by Wang *et al.* in [9] for effective modeling and controlling the complex systems. It consists of Artificial societies (A), Computational experiments (C) and Parallel execution (P). The key idea of ACP is to combine Artificial systems, Computational experiments, and Parallel execution to turn the virtual artificial space into another space for solving complex problems [14]. It is further extended to ACP-based parallel intelligence that is defined as one form of intelligence generated from the interactions and executions between physical and artificial

systems [10]. ACP-based parallel intelligence is becoming an increasingly important research topic and is widely applied such as social computing, traffic management and control, ethylene production management, and autonomous driving [10], [15], [16], [17].

B. Parallel vision framework

ACP methodology is further extended to computer vision community as a Parallel Vision (PV) framework for better perceiving and understanding complex scenes in [18]. Inspired by ACP methodology, PV contains three parts including artificial scenes, computational experiments and parallel execution. From the perspective of PV, the vision models are on-line optimized through parallel evolutionary execution with a virtual/real interactive policy. From the perspective of PV, existing work of learning-by-synthesis [19], [20], [21] is part of PV with respect to artificial scenes and computational experiments. Parallel evolutionary execution aims to construct a closed loop driven by large scale of 'big data' to boost the performance of vision systems. As a result, on-line learning through parallel execution allows the perception model continuously to be optimized.

C. Parallel learning

By taking data, knowledge, and action into a closed loop, parallel learning framework was introduced in [11] to alleviate the limitation in data collecting and policy exploring of existing machine learning framework. Based on ACP methodology, parallel learning framework can capture the mutual dependency between data and action in an artificial system parallel to the physical system from observations. Parallel learning combines descriptive learning, predictive learning and prescriptive learning to effectively collect/generate data and guide the implementation of complex learning systems [12]. In particular, predictive learning urges the decision system to extract informative knowledge based on collected data. For descriptive learning, it forms a self-consistent artificial system to generate new labeled data following the distribution of observed data in real system with minimum human intervention. Moreover, prescriptive learning allows it to guide the system to collect specific data in a supervised manner with descriptive or prior knowledge [22]. Refer to [11], [12] for more details.

III. PARALLEL MEDICAL IMAGING

Conventional medical image analysis framework extracts clinical knowledge from image data in a bottom-up manner where the model learning is driven by data ignoring the prior medical knowledge. However, in the field of medical imaging, domain knowledge plays a critical role for data collection and diagnosis decision support. Properly utilizing medical knowledge in a top-down manner can not only improve the diagnosis but also enhance the interpretability of diagnostic decision. Inspired by the parallel intelligence and the framework of evolutionary systems, we propose a data-knowledge-driven framework termed as parallel medical imaging (PMI) for medical image analysis.

Seeking to provide clarity, we re-illustrate the overall proposed evolutionary framework of PMI as Fig. 2. Two major parts of image data collection and medical knowledge extraction are coupled in PMI by parallel learning in an evolutionary way. The key point is to select and generate image data which are representative to extract desired medical knowledge for final diagnostic decision. Particularly, raw images are collected firstly, followed by variation operators such as augmentation, selection and reproduction with generation for large scale of image data collection. Computational experiments with predictive learning are conducted for data-to-knowledge extraction. In this work, inspired by the key idea of evolutionary optimization through the interactions and executions between physical and artificial systems, we introduce artificial imaging systems (AIS) parallel to physical ones. In AIS, prescriptive learning is adopted to guide the data generation based on the predictively extracted or prior medical knowledge where knowledge-to-data is achieved. This step can also enhance the interpretability of decision. In addition, descriptive learning is adopted in AIS to guide the data selection and generation based on the captured data distribution and knowledge. As a result, final effective diagnosis and prognosis can be achieved through extracted knowledge with enhanced interpretability. Hence, PMI can jointly employ the image data distribution and medical knowledge through bottom-up and top-down learning and inference for final clinical decision. It can reduce the dependence on annotated images and alleviate the limitation of medical interpretation for diagnostic decision. More details are given in the following subsections.

A. Image data collection

For medical imaging, large scale of image data with accurate annotations is critical for the performance of learning-based methods. Parallel imaging framework was introduced in [23] for image generation for PV [18] to tackle the problems of complex vision systems. However, compared with natural image analysis, medical image analysis requires a higher level of expertise for interpretation and labeling. In addition, it is not easy to collect image data from medical institutions or imaging communities since they should be in accordance with the specific security and privacy policies. Moreover, some lesion types and abnormalities have a very low rate of occurrence in the general population [19]. It is therefore more time-consuming and costly to collect effective training data which makes medical imaging remain a challenging task.

In this work, as shown in Fig. 2, from the data perspective of parallel intelligence [10], [23], real medical images with annotations are kind of 'small data'. Through effective reproduction and variation operation such as conventional augmentation, active selection, and generation by introduced artificial imaging systems, a set of 'big data' with real and synthetic images is formed for conducting computational experiments for medical knowledge extraction.

1) *Augmentation and selection of real images*: In the step of image data collection, small and/or imbalanced real images for training can be augmented. Similar to conventional methods, rotation, scaling, flipping, translation and adding noise

can be applied for medical image augmentation [4], [20], [24]. Examples for skin lesion augmentation are illustrated in Fig.3.

The performance of learning-based methods for medical image analysis not only depends on the size but also the representativeness of labeled images. However, due to a lack of standardization in imaging and acquisition for medical images, selecting representative training samples for computational experiments remains a challenging task. In this framework, suitable selection of real images is performed to address this challenge. To this end, simple unsupervised/semi-supervised can be applied for data selection. In addition, active learning that aims at using limited medical images for disease classification can be developed. Active learning iteratively selects the most informative samples through the interaction between experts and computer. In active learning, the key is to develop a criterion for uncertainty in sample selection process. In [25], *entropy* and *diversity* are adopted to indicate the power of candidate patches in elevating the performance of current CNN model. For the i -th patch of k -th candidate denoted by x_k^i , the prediction is p_k^i and its entropy is formulated as below:

$$e(x_k^i) = - \sum_{c=1}^N p_k^{i,c} \log p_k^{i,c}, \quad (1)$$

where $c = 1, 2, \dots, N$ is the possible class. The *diversity* between sample patch x_k^i and x_k^j is defined as below:

$$d(x_k^i, x_k^j) = \sum_{c=1}^N (p_k^{i,c} - p_k^{j,c}) \log \frac{p_k^{i,c}}{p_k^{j,c}}. \quad (2)$$

According to [25], sample patch with higher entropy and higher diversity are expected to be selected to elevate the model performance. Another uncertainty criterion in sample selection is breaking ties (BT) heuristic that ranks the candidate samples by the posterior probabilities [26]. The decision criterion of BT heuristic for measuring the uncertainties of samples is the difference between the two highest posterior probabilities as below:

$$\zeta(x_k) = \max_{c \in N} p(y_k = c | x_k) - \max_{c \in N \setminus c^+} p(y_k = c | x_k), \quad (3)$$

where $p(y_k = c | x_k)$ is the posterior of k -th sample x_k with label y_k belonging to the class c , and c^+ denotes the class label with maximal probability. If $\zeta(x_k)$ is small, the corresponding sample is informative to be selected.

2) *Generation of synthetic images*: To utilize the medical domain knowledge, we propose to apply descriptive learning and design artificial imaging systems parallel to real imaging systems that can generate synthetic and specific medical images following the distribution of real ones. Many techniques for generating new synthetic medical images in our proposed framework of artificial imaging systems can be applied. They typically fall into three categories. In the first one, new lesions are mathematically simulated based on various deformation, followed by inserting into the raw projection data or reconstructed clinical images, such as mammography [28], [27] and lung nodules [29], [30]. An example from [27] is illustrated in Fig.4. To assure the realism of the characteristics of the artificial samples, real lesions can be extracted and inserted to the same or different images [31].

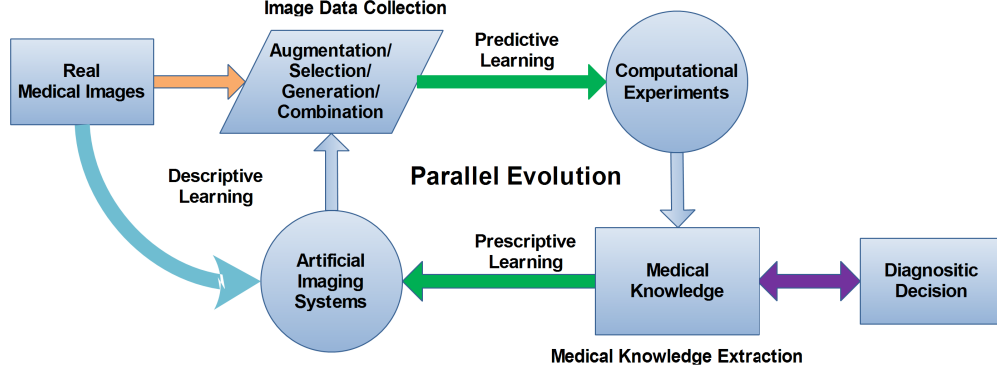


Fig. 2. Evolutionary framework of PMI with parallel learning.

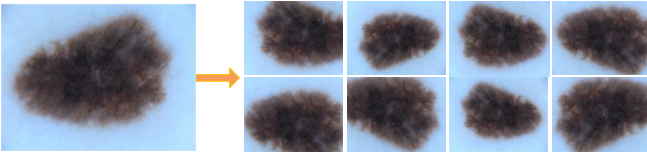


Fig. 3. Skin lesion augmentation through rotation, flipping and cropping.

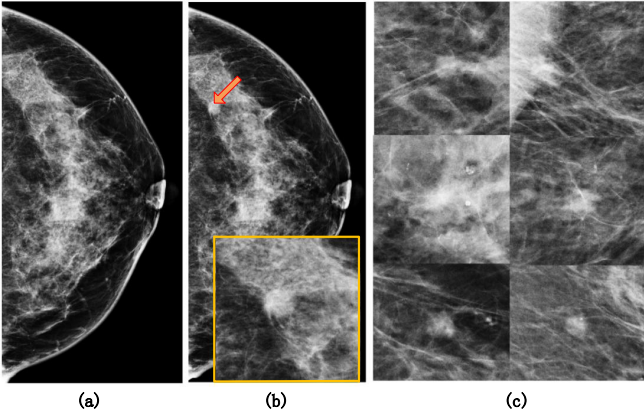


Fig. 4. Synthesis by insertion. (a) Normal mammogram, (b) Insert mass, (c) Simulated lesions by diffusion limited aggregation [27].

In the second one, virtual images are simulated through computer graphics based on abstraction of the prior medical knowledge. Particularly, synthetic images are generated by selection of simulation parameters of models under controlled hypothetical imaging conditions [32]. In [33], [34], computerized phantom (eXtended CArdiac-Torso, XCAT) is served as a virtual patient, followed by feeding into artificial imaging system with an accurate computerized model, which can generate photorealistic CT image data with patient-quality as show in Fig.5.

In the third one, generative models for image synthesis can be learned in the artificial imaging systems. In [35], the authors propose a model of fully convolutional neural networks for MRI synthesis. This model learns to input modalities into a shared modality-invariant latent space which allows it to benefit from additional input modalities and robust to missing

data. Recently, adversarial learning for the generative model is widely used for medical image synthesis [20], [36], [37], [38], [39]. GANs [40] are a specific framework of a generative model that aims to implicitly learn the data distribution p_{data} from real image samples to generate new samples from learned distribution. GANs contains a generator G and a discriminator D . G aims to synthesize fake samples and D aims to discriminate between real and fake images. For the input x , $D(x)$ represents the probability of being a real image. For the input z from a simple distribution p_z , $G(z)$ represents the generated synthetic image. The basic loss function for adversarial networks is a two-player minimax game formulated as below:

$$\min_G \max_D \{f(D, G) = \mathbb{E}_{x \sim p_{data}(x)} [\log D(x)] + \mathbb{E}_{z \sim p_z(z)} [\log(1 - D(G(z)))]\}, \quad (4)$$

where \mathbb{E} represents the expectation. We can rewrite this loss function as below:

$$f_S = \mathbb{E}[\log P(S = real|X_{real})] + \mathbb{E}[\log P(S = fake|X_{fake})], \quad (5)$$

where $P(S|X) = D(X)$ and $X_{fake} = G(z)$. And D is trained to maximize f_S which denotes it assigns to the correct image source. G is trained to minimize the second term of f_S . In ACGAN[41], in addition to f_S , a term of log-likelihood with correct class is defined by:

$$f_Y = \mathbb{E}[\log P(Y = y|X_{real})] + \mathbb{E}[\log P(Y = y|X_{fake})], \quad (6)$$

where Y is the possible label, $P(Y|X) = D(X)$ and $P(S|X) = D(X)$ denote a probability distribution over class labels and sources, respectively. D is trained through maximizing $f_Y + f_S$ and G is trained through maximizing $f_Y - f_S$. It is noticing that $X_{fake} = G(y, z)$ in ACGAN. ACGAN [41] is applied in [20] for generating synthetic medical images. Baur and Albarqouni improve LAPGAN in [36] to generate high resolution lesion images as illustrated in Fig.6. In [38], Ben Taieb and Hamarneh present a combination of generative, discriminative and task specific networks for histopathology normalization. In this work, effective generator of GANs can be utilized into the step of artificial imaging systems.

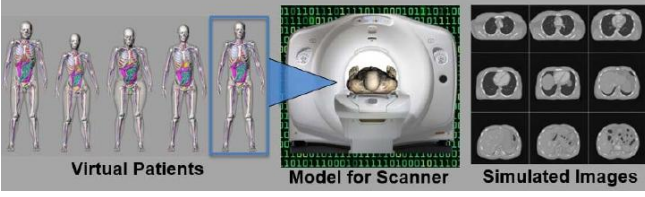


Fig. 5. Computed tomography (CT) synthesis through an XCAT phantom[33].

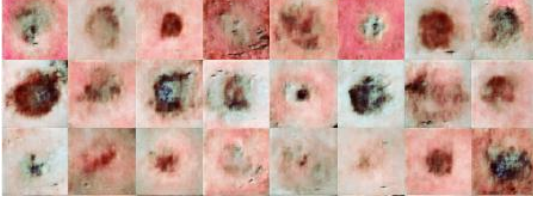


Fig. 6. Synthesized images with skin lesions based on GAN [36]

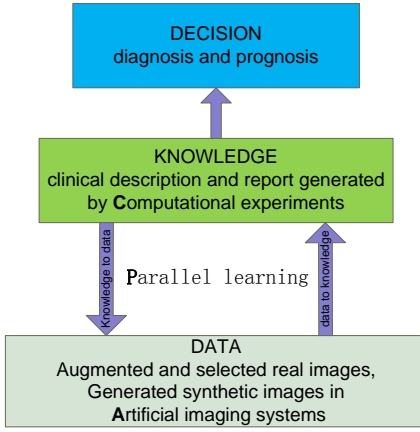


Fig. 7. Data-knowledge-driven for decision pyramid in PMI.

B. Medical knowledge extraction

Conventional methods of turning data into medical knowledge relied on visual analysis and interpretation by a domain expert or radiologist in order to find useful patterns in data for decision support [42]. As pointed in radiomics [43], [44], effective conversion of images to mineable data supports the diagnostic decision. In this work, after effective image collection, computational experiments with predictive learning are conducted to extract 'small' medical knowledge in PMI. Hence, medical knowledge extraction from image also is a part of radiomics.

For this research topic in parallel medical imaging, any information about the patient's ultrasonic signs, X-ray findings and other related image-based medical descriptions are termed as 'symptom'. Computational experiments with predictive learning try to perform effective diagnosis. To achieve this goal, we have to extract medical knowledge by studying the relationships of obligatory proving or excluding symptoms for diagnosis in books and in practical experience. These certain information about relationships that exist between symptoms and diagnoses, symptoms and symptoms, diagnoses and diagnoses and more complex relationships of combinations of

symptoms and diagnoses to a symptom or diagnosis are formalizations of what is called medical knowledge [45].

Predictive learning was originally inspired by the cognitive psychology study that how children construct knowledge of the world by interacting with it [17]. In the step of computation experiments, we perform predictive learning for diagnosis model from collected image data for decision support. It can be simplified as part of medical knowledge extraction from image data. Conventional data-driven machine learning techniques especially deep learning models can be learned to address knowledge extraction in PMI. In general, computational experiments in PMI include detection, segmentation, classification, or relationship caption for decision support for clinical applications. The detection model extracts the knowledge of rough location and size of the lesion area. Subsequently, the segmentation model extracts the detailed shape and margin information of the lesion. Finally, the knowledge of pathological types and assessment categories are obtained through the classification task. Sometimes we need to capture the relationship between symptoms and diagnosis.

C. Parallel evolution with parallel learning

In subsection III-A2, we have introduced some techniques that can be applied in artificial imaging systems to utilize the domain knowledge. In this subsection, we further discuss the details of parallel learning that is incorporated in PMI to achieve evolutionary optimization.

As shown in Fig. 7, we introduce parallel learning to take advantage of bidirectional relationship between medical image data and clinical description/representation of medical knowledge. Predictive learning of parallel learning to achieve data-to-knowledge extraction in a bottom-up manner is discussed in last subsection III-B. Different from traditional diagnosis of treating medical images as pictures intended solely for visual interpretation, conversely, through a top-down inference, the extracted medical knowledge can be used for guiding the image generation as well as increasing the interpretability of future diagnosis. As described in subsection II-C, we employ descriptive and prescriptive learning of parallel learning to improve the model generalization ability and enhance the interpretation for medical diagnosis decision.

1) *Descriptive learning*: Descriptive learning aims to devise models to explain and predict learning results [22]. In this work, it urges the introduced artificial imaging system to generate new images that follow the distribution of observed data. For PMI in this paper, the key idea of descriptive learning is to model the image distribution inside the designed artificial imaging systems, perception and reasoning based on the observation in real world. The descriptive learning process allows for learning features from unlabeled data in a semi-supervised or unsupervised manner. Adversarial learning of GAN for image generation can be seen as a special case where the objective is to minimize the difference of distribution for real and generated images.

2) *Prescriptive learning*: According to the definition in [22], prescriptive learning is concerned with guidelines that describe what to do in order to generate specific outcomes.

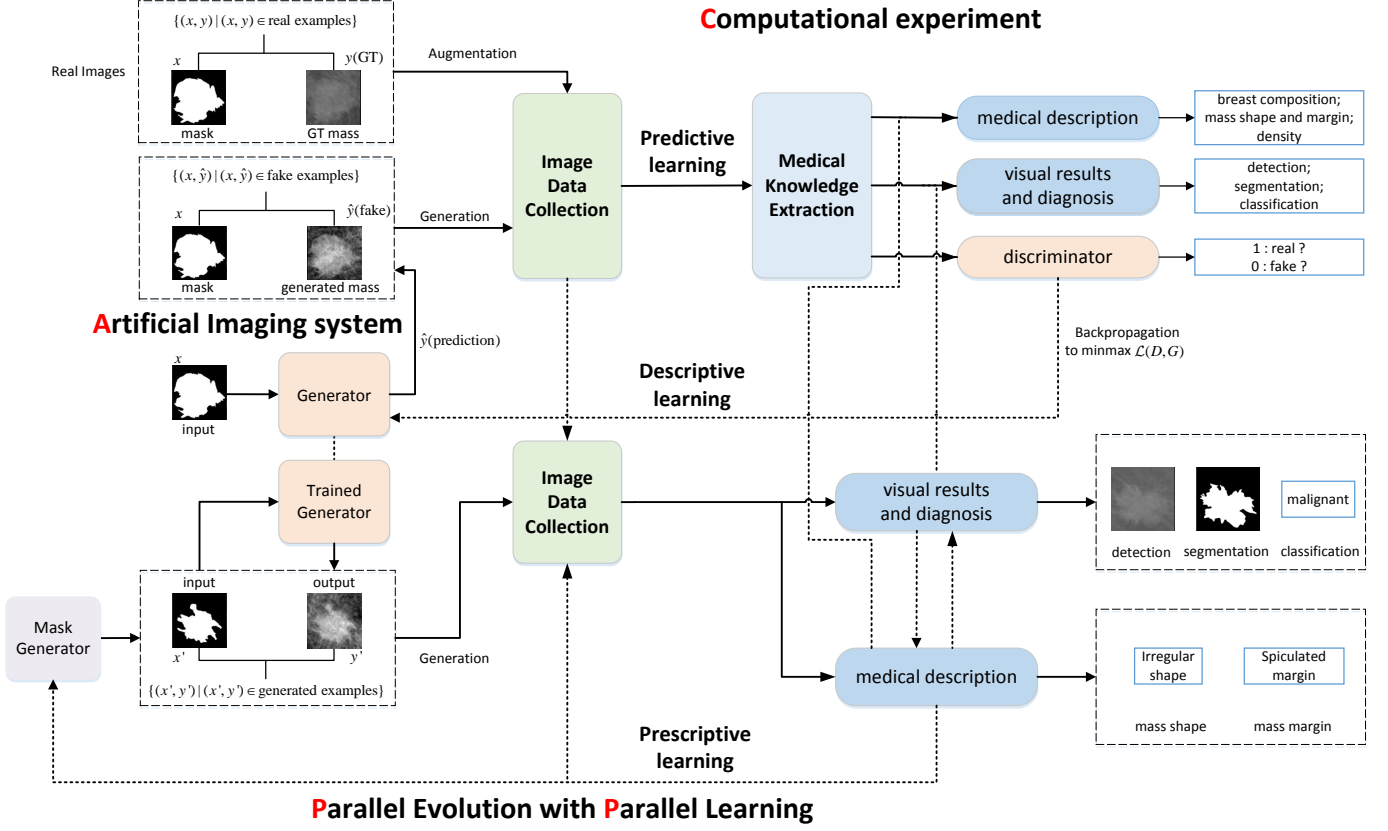


Fig. 8. GANs-based PMI framework for breast mass analysis.

They are often based on descriptive theories or derived from prior knowledge. In this work, we achieve knowledge-to-data generation and enhance interpretability through prescriptive learning of parallel learning. According to the ACP methodology, we perform parallel execution with prescriptive learning to guide the artificial medical imaging systems to collect specific representative image data based on the extracted or prior medical descriptions and knowledge. For instance, based on the prior medical knowledge that mammograms with spiculated and irregular mass are mostly malignant, we can prescriptively generate various irregular and spiculated mass image with associated pleomorphic calcifications for malignant breast cancer analysis in mammograms [46]. As a result, visual interpretation on the diagnostic results is enhanced through prescriptive learning which effectively capture the relationship between malignancy and interpretability.

IV. CASE STUDY OF MAMMOGRAM

To validate the effectiveness of proposed PMI framework, we further perform a case study of mammogram analysis in this section. The clinical descriptive details from standard Breast Imaging Reporting and Data System (BI-RADS) [47] are illustrated in Table.I and Table.II that explicitly inform the domain knowledge description. Similar to the work in [46] as shown in Fig.9, after capturing the relationship between the malignancy and clinical description as listed in Table II, diagnosis with interpretability can be enhanced. For visual

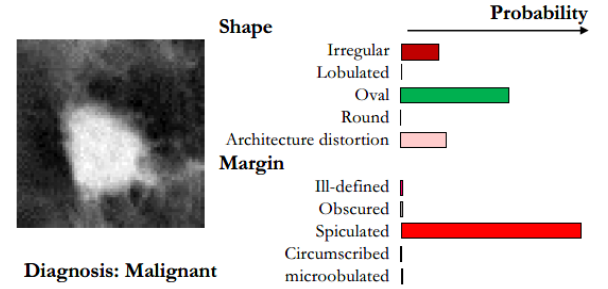


Fig. 9. Clinical description in mammography lexicon with interpretability for breast mass analysis [46].

results and diagnosis, the visual diagnosis models is trained for visual information extraction like detection, segmentation and classification. Due to page limitation, we only study the problem of local X-ray breast mass classification (benign/malignant) for diagnosis. Built upon PMI, we perform an implementation based on GANs with image data collection, medical description of knowledge and parallel evolutionary learning. The overall framework is illustrated in Fig. 8. More details are given in following subsections.

A. Dataset and Evaluation Criteria

Experiments are conducted in the public available dataset of INbreast [48] which is one of most widely used for

TABLE I
CLINICAL DESCRIPTION FOR MAMMOGRAPHY: BREAST COMPOSITION, MASS SHAPE AND MARGIN, DENSITY.

Breast composition	a.	The breast are almost entirely fatty;
	b.	There are scattered areas of fibroglandular density;
	c.	The breasts are heterogeneously dense, which may obscure small masses;
	d.	The breasts are extremely dense, which lowers the sensitivity of mammography.
masses	shape	Oval; Round; Irregular.
	Margin	Circumscribed; Obscured; Microlobulated; Indistinct; Spiculated.
	Density	High density; Equal density; Low density; Fat-containing.

TABLE II
BREAST IMAGING REPORTING AND DATA SYSTEM (BI-RADS)
ASSESSMENT CATEGORIES

Category	Description
0	Needs additional imaging evaluation and/or prior mammograms for comparison.
1	Negative.
2	Benign finding(s).
3	Probably benign finding(s). Short-interval follow-up is suggested.
4	Suspicious anomaly. Biopsy should be considered.
5	Highly suggestive of malignancy. Appropriate action should be taken.
6	Biopsy proven malignancy.

mammogram analysis. The INbreast dataset is created by the Breast Research Group, INESC Porto, Portugal, and consists of a total of 115 cases (410 images) including 107 images of cancer and 236 images of normal breast. In this work, local ROI of 107 mass images with cancers are cropped into 256×256 pixels along with the corresponding mask applying the same operation. A total of 112 squared mass images are obtained because some of these cases have more than one mass and they are annotated (benign or malignant) according to the Breast Imaging Reporting and Data System (BI-RADS), which is a standard criteria developed by the American College of Radiology (ACR)[48] as listed in Table II. In this work, 36 masses with BI-RADS Category $\in \{2, 3\}$ are categorized as benign, and 76 masses with BI-RADS Category $\in \{4, 5, 6\}$ are categorized as malignant.

The performance is analyzed by measurement metrics in the binary classification problem, including overall accuracy, TP and TPR, FN and FNR, TN and TNR, FP and FPR. TP, TN, FP, and FN are defined the number of true positive, true negative, false positive, and false negative detections, respectively. The rest metrics are defined in the following equations:

$$\begin{aligned}
 \text{Accuracy} &= \frac{\text{TP} + \text{TN}}{\text{TP} + \text{FN} + \text{TN} + \text{FP}}, \\
 \text{FNR} &= \frac{\text{FN}}{\text{TP} + \text{FN}}, \quad \text{TPR} = \frac{\text{TP}}{\text{TP} + \text{FN}}, \\
 \text{FPR} &= \frac{\text{FP}}{\text{FP} + \text{TN}}, \quad \text{TNR} = \frac{\text{TN}}{\text{FP} + \text{TN}}.
 \end{aligned} \tag{7}$$

A good performance of classification is achieved with high

accuracy, TPR(TP) and TNR(TN) as well as low FNR(FN) and FPR(FP). Moreover, ROC (Receiver Operating Characteristic) curves and their AUCs (Area Under the Curve) is also used to evaluate the performance of classification model. ROC curve is produced by FPR (horizontal axis) and TPR (vertical axis). A better performance is achieved with a larger AUC.

B. Implementation

1) *Predictive learning for malignancy extraction:* Firstly, conventional augmentation including rotation and flipping on real images are performed for training. In particular, 64 pairs of real mass images (a mass image y and a corresponding mask x that incorporates shape and margin information of masses) are randomly selected to augment into 512 pairs of images for training the descriptive models. The rest 48 pairs of real images are used for testing. In this work, we introduce a CNN architecture and perform predictive learning to classify the mass image with corresponding masks as malignant or benign in the step of computational experiments. The CNN architecture with details is exhibited in Fig. 10. Cross Entropy is used as a loss function which is computed by:

$$L = -\frac{1}{n} \sum_{i=1}^n [l^i \log(p^i) + (1 - l^i) \log(1 - p^i)], \tag{8}$$

where (x, y) denotes the pair of input, n is the number of training samples, l represents actual label with 1 denoting malignancy and 0 for the benign, p is the predicted value.

2) *Descriptive learning for synthetic data generation:* The quantity of available medical image data is always small. Combination of large scale of generated synthetic data and the 'small' real data has shown to be helpful in data-driven optimization problem [49]. In this work, inspired by the idea that adversarial learning is a special case of parallel learning [11], we introduce a generative adversarial network structure for descriptive mass images generation in the artificial imaging system. Specifically, a conditional GAN (cGAN) structure [50] is designed for generation from given binary masks x which already incorporate the shape and margin descriptive information. The generator G and discriminator D of GAN are trained for learning the distribution of mass images as well as a mapping $G : \{x, z\} \rightarrow y$ between masks x , random noise z , and real mass images y . Similar to [50], a U-net structure is introduced as the generator and a PatchGAN architecture is

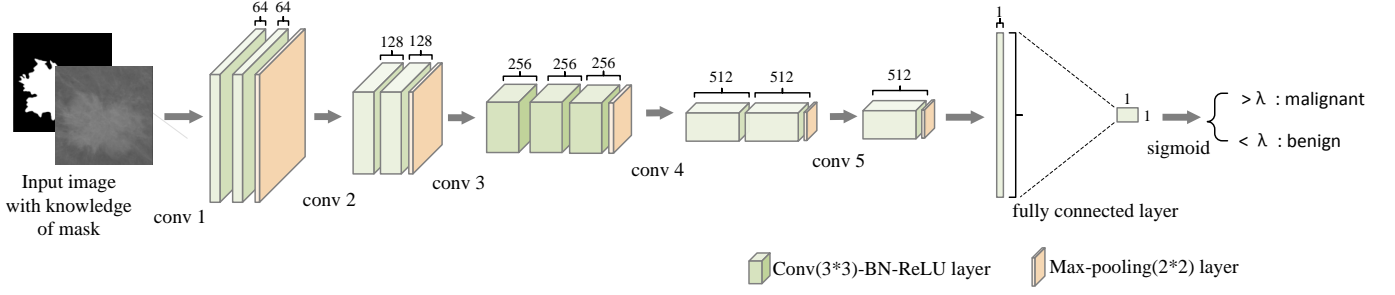


Fig. 10. CNN architecture for the mass classification: Dropout (0.3) is used before the fully connected layer.

introduced as the discriminator. Refer [50] for more details. To learn a effective generator G in artificial imaging systems based on adversarial learning, we set the objective function as below:

$$G^* = \arg \min_G \max_D \mathbb{E}_{x,y} [\log D(x,y)] + \mathbb{E}_{x,z} [\log(1 - D(x, G(x,z)))] + \mathbb{E}_{x,y,z} [\|y - G(x,z)\|_1]. \quad (9)$$

And the discriminator D is learned as described in [40] that aims to distinguish the input as real or synthetic. G and D are alternatively optimized until convergence. Then we can acquire the effective generator which is part of artificial imaging system performing synthetic data generation. The combination of 'small' set of real images and 'big' set of synthetic ones forms a large scale of training samples that can be further fed into predictive learning for 'small' knowledge extraction.

3) *Prescriptive learning for specific data generation and selection*: As shown in Fig. 7, the workflow of data-to-knowledge is a bottom-up manner with the medical visual and descriptive knowledge learning from existing training samples. Conversely, through the knowledge-to-data inference in a top-down manner, the medical knowledge is used for guiding the image augmentation, selection and generation, and enhancing the interpretability of diagnosis. In this case, prescriptive learning is adopted to generate specific malignant/benign mask images with corresponding shape and margin based on the descriptively extracted knowledge or prior medical knowledge. To this end, a deep convolutional generative adversarial network (DCGAN) [51] is implemented to generate the specific binary mask. To utilize the medical knowledge that malignant mass is also with irregular shape and spiculated margin and benign mass with oval shape and circumscribed margin [46], [47], we train two generators separately through adversarial learning in prescriptive scheme for benign and malignant binary mask generation. In this work, 37 benign and 75 malignant masks are augmented into 296 benign and 600 malignant masks for training the DCGAN model. 262 benign and 409 malignant masks are obtained and used to generate the corresponding mass images through the previously trained cGAN model in the step of descriptive learning. Some generated masks are shown in Fig. 11. Hence, a generative model from introduced DCGAN can achieve knowledge-driven data generation.

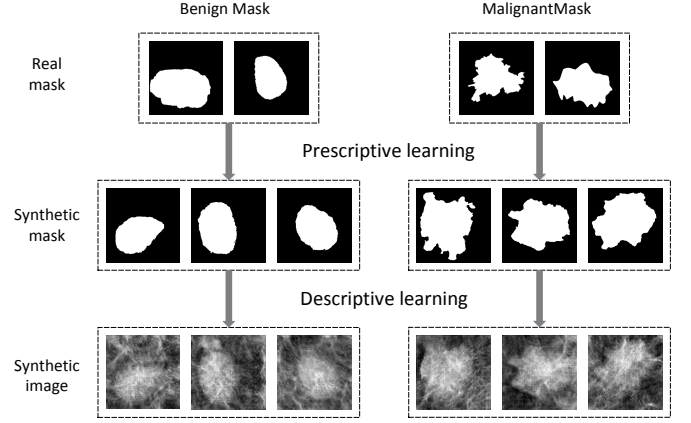


Fig. 11. Qualitative results for generating binary masks and corresponding mass images by our proposed framework.

By feeding the generated benign and/or malignant binary mask into artificial imaging systems through descriptive learning, more specific realistic-looking lesion images from interpreting conditions such as margin and shape of masses can be collected. Then we can extract more suitable medical knowledge through predictive learning in a data-driven way for final diagnosis. The overall framework jointly employ the image data collection and medical knowledge extraction in a closed loop through data-to-knowledge predictive learning and knowledge-to-data prescriptive learning. Parallel data-knowledge-driven evolutionary optimization is achieved.

C. Experimental Results

For the experiments, 4-fold cross-validation tests were carried out, which ensures that the samples are tested equally to prevent any bias error. The real samples are augmented into 512 samples and divided into four folds. Each fold contains 128 real samples with 48 benign masses and 80 malignant masses. Three folds are for training and the rest for testing. Firstly, we perform predictive binary classification on real data using the CNN model where we term it as *Pred (baseline)*. Then we apply the descriptively trained cGAN to generate synthetic mass images. In addition, we perform predictive learning using CNN on the combination of real and synthetic images for binary classification where we term it as *Pred+Desc*. Finally, to validate the effectiveness of utilizing domain knowledge by prescriptive learning, we apply the

TABLE III
MEASUREMENT METRICS OF CLASSIFICATION VIA PROPOSED CNN TRAINED ON REAL AND COLLECTED SETS IN PMI OVER 4-FOLD CROSS VALIDATION ON THE TEST SETS OF THE INBREAST DATASET.

Test Fold	Learning Method	Measurement metrics				
		Accuracy	TPR(TP)	FNR(FN)	TNR(TN)	FPR(FP)
1 st fold	<i>Pred (baseline)</i>	90.63%	85.00%(68)	15.00%(12)	100%(48)	0%(0)
	<i>Pred+Desc</i>	94.53%	91.25%(73)	8.75%(7)	100%(48)	0%(0)
	<i>Pred+Desc+Pres</i>	99.22%	98.75%(79)	1.25%(1)	100%(48)	0%(0)
2 nd fold	<i>Pred (baseline)</i>	80.47%	75.00%(60)	25.00%(20)	89.58%(43)	10.42%(5)
	<i>Pred+Desc</i>	84.38%	81.25%(65)	18.75%(15)	89.58%(43)	10.42%(5)
	<i>Pred+Desc+Pres</i>	87.5%	90.00%(72)	10.00%(8)	83.33%(40)	16.67%(8)
3 rd fold	<i>Pred (baseline)</i>	74.22%	80.00%(64)	20.00%(16)	64.58%(31)	35.42%(17)
	<i>Pred+Desc</i>	77.34%	76.25%(61)	23.75%(19)	79.17%(38)	20.83%(10)
	<i>Pred+Desc+Pres</i>	78.91%	73.75%(59)	26.25%(21)	87.5%(42)	12.5%(6)
4 rd fold	<i>Pred (baseline)</i>	94.53%	91.25%(73)	8.75%(7)	100%(48)	0%(0)
	<i>Pred+Desc</i>	97.66%	96.25%(77)	3.75%(3)	100%(48)	0%(0)
	<i>Pred+Desc+Pres</i>	95.31%	100%(80)	0%(0)	87.5%(42)	12.5%(6)
Average	<i>Pred (baseline)</i>	84.96%	82.81%	17.19%	88.54%	11.46%
	<i>Pred+Desc</i>	88.48%	86.25%	13.75%	92.19%	7.81%
	<i>Pred+Desc+Pres</i>	90.24%	90.63%	9.37%	89.58%	10.42%

introduced DCGAN to generate benign and malignant binary masks followed by synthetic mass image generation from masks through descriptively trained cGAN. As a result, a synthetic dataset with 1040 benign samples and 1636 malignant samples are formed that is combined with three folds of real images to form a new collected set for training the CNN model. We term this procedure as *Pred+Desc+Pres*. All the testings are conducted on the same real data with the same training parameters setting. Experimental results are listed in Table III and ROC curves are shown in Fig. 12.

As shown in Table III, conventional CNN trained on real images with augmentation for malignancy classification achieves an average accuracy of 84.96%. After descriptive adversarial learning for synthetic mass image generation for training, its average accuracy improves to 88.48%. In addition, specific type of binary masks and related mass images are prescriptively generated in a knowledge-driven way to enlarge the variations of training data. In this step, medical knowledge such as that benign mass always arise with oval shape and circumscribed margin, while the malignant mass along with irregular shape and spiculated margins are utilized for data generation and collection. Through such evolutionary optimization on existing real data, an average accuracy of 90.24% is further achieved. The CNN trained on the descriptive and prescriptive generated data performs better with higher classification accuracy than the model trained on real set under the same testing set and training parameters setting. As shown in Fig. 12, the ROC curves also demonstrate the effectiveness of proposed optimization framework with AUCs of 85.68%, 89.22%, and 90.11%, respectively. By further investigation,

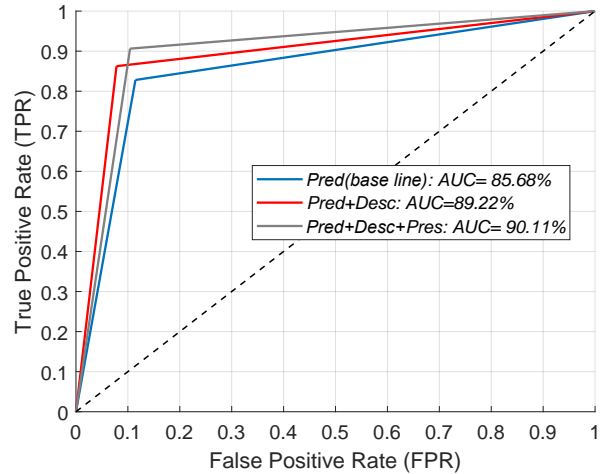


Fig. 12. The performance of CNN trained on the original real and collected sets (combination of real and synthesized by generator in artificial imaging system) in terms of ROC curves on the test sets.

predictive learning from descriptively generated samples in artificial imaging system can boost the performance in computational experiments for medical knowledge extraction. Generating the desired binary mask of masses for image synthesis based on the prior medical knowledge through prescriptive learning in our proposed GANs-based PMI framework further improve the accuracy and it can enhance the interpretability for diagnosis. This GANs-based PMI framework can be easily generalized to other task of medical imaging such as skin

cancer analysis. In summary, our proposed data-knowledge evolutionary framework is capable of describing, predicting, and prescribing the correlation between the image data and medical knowledge in real complex imaging systems.

V. CHALLENGES AND FUTURE RESEARCH DIRECTIONS IN PMI

A. Medical image data sharing

Medical imaging is not only confined to diagnostic radiology because pathology, dermatology and related case reports are increasingly creating and storing in format of digital images. Although we can generate large scale of synthetic image data through the proposed parallel medical imaging framework for training models, it is still limited to cover all the variations in real scenarios. There is rising demand for medical image data sharing for both healthcare organizations and individuals. However, there are many issues to be addressed for image data sharing in medical domain such as data recording methods, different imaging standards from different manufacturers, difficulties in culture and language, data security and safety, and individual privacy policy. The CAT system [44] are presented to link multiple centres via learning connectors which are interface where machine learning algorithms learn models locally. Hence, the private information is protected in the local institute.

Blockchain technology also have great potential for addressing above issues in medical imaging which will be future research directions [52], [53], [54], [55], [56]. A blockchain for cross-domain image sharing is introduced as a distributed data store to establish a ledger of radiological studies and patient-defined access permissions in [52]. Blockchain-based system enable a patient-centric approach and could enhance security and reliability of individual data since patients have control over their own medical images with respect to records. The ACP-based blockchain framework [56], [57] can be further extended to parallel medical imaging to eliminate third-party access to protected health information, satisfy many criteria of an interoperable health system, and also readily generalize to domains beyond medical imaging.

B. Medical knowledge representation

As described in subsection III-B, information about the relationships between symptoms and diagnoses, symptoms and symptoms, diagnoses and diagnoses can be termed as medical knowledge. To date, most researches mainly try to capture relationship between symptoms and diagnoses or symptoms and symptoms. For PMI, as aforementioned case study, natural language description in Table I for specific medical knowledge with binary label to denote existing or not is adopted for enhancing interpretability. In addition, visual results such as the lesion location in a medical image and related disease entities are also medical knowledge representations. However, the ideal representation of medical knowledge such as uncertainty between symptoms and diagnoses is to set an occurrence probability. Intuitionistic fuzzy set analysis [58], [59], [60], [61] allows medical knowledge representation at varying levels of certainty. Qualitative description by means of natural

language using theory of fuzzy sets is adapted to express ambiguous medical knowledge [45], [62]. Linguistic terms (such as {never,...,always}) between diagnosis and symptoms are used to express physicians' uncertainty.

C. Interpretability

In conventional data mining domain, the machine learning technology, especially deep models, have achieved impressive results and even exceeded human performance in visual tasks in accuracy. However, except for accuracy in medical imaging, it is also necessary to consider the interpretability where the produced or predicted results are explainable to others [63].

As proposed in PMI, although predictive and prescriptive learning of parallel learning with quantitative description of medical knowledge can enhance the interpretability, it is still limited to overcome the explainability difficulties in medical domain since we can not list all the quantitative feature description with respect to specific disease. Except for the image data, we can learn from related text reports to enhance the interpretability. A larger amount of knowledge is represented in textual form [64]. We can construct specific knowledge graph from training pairs of image and related text reports to underpin the diagnosis decision with reasons that are explainable.

VI. CONCLUSION

In this paper, we proposes an evolutionary data-knowledge-driven framework termed as Parallel Medical Imaging for vision-based medical image analysis. Artificial imaging systems with descriptive learning allows to collect large scale of real and synthetic images for training and evaluating the models in the computational experiments. With a knowledge-to-data in a top-down manner through prescriptive learning, we can select and generate specific image data based on the prior or extracted medical domain knowledge. With a data-to-knowledge in a bottom-up inference through predictive learning, we can extract medical knowledge for clinical diagnostic supporting systems. Through parallel evolution, 'large' scale of medial image data are collected from 'small' set of real images, followed by 'small' intelligence with interpretable medical knowledge extraction. Experimental results from the case study also demonstrate that parallel data-knowledge-driven evolutionary scheme alleviates the limitations of small quantity of available medical images and enhance the interpretability for final diagnosis and prognosis with more descriptive information.

Future work will focus on expanding proposed PMI framework beyond diagnosis decision support in medical imaging. For the foreseeable future, the field of parallel medical imaging has tremendous potential to supplement and verify the work of clinicians, train radiologists to be more skilled, perform the surgical planning, apply intra-operative navigation, give personalized medicine recommendation, and visualize medical images with interpretable masks, particularly in the complex field of imaging analytics with complicated diseases.

REFERENCES

- [1] D. Shen, G. Wu, and H.-I. Suk, "Deep learning in medical image analysis," *Annual review of biomedical engineering*, vol. 19, pp. 221–248, 2017.
- [2] Z. Hu, J. Tang, Z. Wang, K. Zhang, L. Zhang, and Q. Sun, "Deep learning for image-based cancer detection and diagnosis survey," *Pattern Recognition*, 2018.
- [3] H. Haenssle, C. Fink, R. Schneiderbauer, F. Toberer, T. Buhl, A. Blum, A. Kalloo, A. Hassen, L. Thomas, A. Enk *et al.*, "Man against machine: diagnostic performance of a deep learning convolutional neural network for dermoscopic melanoma recognition in comparison to 58 dermatologists," *Annals of Oncology*, 2018.
- [4] A. Esteva, B. Kuprel, R. A. Novoa, J. Ko, S. M. Swetter, H. M. Blau, and S. Thrun, "Dermatologist-level classification of skin cancer with deep neural networks," *Nature*, vol. 542, no. 7639, p. 115, 2017.
- [5] J. I. Orlando, E. Prokofyeva, M. del Fresno, and M. B. Blaschko, "An ensemble deep learning based approach for red lesion detection in fundus images," *Computer methods and programs in biomedicine*, vol. 153, pp. 115–127, 2018.
- [6] B. E. Bejnordi, M. Veta, P. J. Van Diest, B. Van Ginneken, N. Karssemeijer, G. Litjens, J. A. Van Der Laak, M. Hermesen, Q. F. Manson, M. Balkenhol *et al.*, "Diagnostic assessment of deep learning algorithms for detection of lymph node metastases in women with breast cancer," *Jama*, vol. 318, no. 22, pp. 2199–2210, 2017.
- [7] M. A. Al-antari, M. A. Al-masni, M.-T. Choi, S.-M. Han, and T.-S. Kim, "A fully integrated computer-aided diagnosis system for digital x-ray mammograms via deep learning detection, segmentation, and classification," *International Journal of Medical Informatics*, vol. 117, pp. 44–54, 2018.
- [8] W. Zhu, C. Liu, W. Fan, and X. Xie, "Deeplung: Deep 3d dual path nets for automated pulmonary nodule detection and classification," *arXiv preprint arXiv:1801.09555*, 2018.
- [9] F.-Y. Wang, "Parallel system methods for management and control of complex systems [j]," *Control and Decision*, vol. 5, p. 001, 2004.
- [10] F.-Y. Wang, X. Wang, L. Li, and L. Li, "Steps toward parallel intelligence," *IEEE/CAA Journal of Automatica Sinica*, vol. 3, no. 4, pp. 345–348, 2016.
- [11] L. Li, Y. Lin, N. Zheng, and F.-Y. Wang, "Parallel learning: a perspective and a framework," *IEEE/CAA Journal of Automatica Sinica*, vol. 4, no. 3, pp. 389–395, 2017.
- [12] L. Li, N.-N. Zheng, and F.-Y. Wang, "On the crossroad of artificial intelligence: A revisit to alan turing and norbert wiener," *IEEE transactions on cybernetics*, 2018.
- [13] H. Wang, Y. Jin, and J. O. Jansen, "Data-driven surrogate-assisted multiobjective evolutionary optimization of a trauma system," *IEEE Trans. Evolutionary Computation*, vol. 20, no. 6, pp. 939–952, 2016.
- [14] F.-Y. Wang, J. J. Zhang, X. Zheng, X. Wang, Y. Yuan, X. Dai, J. Zhang, and L. Yang, "Where does alphago go: from church-turing thesis to alphago thesis and beyond," *IEEE/CAA Journal of Automatica Sinica*, vol. 3, no. 2, pp. 113–120, 2016.
- [15] F.-Y. Wang, "Parallel control and management for intelligent transportation systems: Concepts, architectures, and applications," *IEEE Transactions on Intelligent Transportation Systems*, vol. 11, no. 3, pp. 630–638, 2010.
- [16] F.-Y. Wang and P. K. Wong, "Intelligent systems and technology for integrative and predictive medicine: An acp approach," *ACM Transactions on Intelligent Systems and Technology (TIST)*, vol. 4, no. 2, p. 32, 2013.
- [17] F.-Y. Wang, N.-N. Zheng, D. Cao, C. M. Martinez, L. Li, and T. Liu, "Parallel driving in cpss: a unified approach for transport automation and vehicle intelligence," *IEEE/CAA Journal of Automatica Sinica*, vol. 4, no. 4, pp. 577–587, 2017.
- [18] K. Wang, C. Gou, N. Zheng, J. M. Rehg, and F.-Y. Wang, "Parallel vision for perception and understanding of complex scenes: methods, framework, and perspectives," *Artificial Intelligence Review*, pp. 1–31, 2017.
- [19] A. Pezeshk, N. Petrick, W. Chen, and B. Sahiner, "Seamless lesion insertion for data augmentation in cad training," *IEEE transactions on medical imaging*, vol. 36, no. 4, pp. 1005–1015, 2017.
- [20] M. Frid-Adar, I. Diamant, E. Klang, M. Amitai, J. Goldberger, and H. Greenspan, "Gan-based synthetic medical image augmentation for increased cnn performance in liver lesion classification," *arXiv preprint arXiv:1803.01229*, 2018.
- [21] C. Gou, Y. Wu, K. Wang, K. Wang, F.-Y. Wang, and Q. Ji, "A joint cascaded framework for simultaneous eye detection and eye state estimation," *Pattern Recognition*, pp. 23–31, 2017.
- [22] C. Ullrich, "Descriptive and prescriptive learning theories," in *Pedagogically Founded Courseware Generation for Web-Based Learning*. Springer, 2008, pp. 37–42.
- [23] K. Wang, Y. Lu, Y. Wang, Z. Xiong, and F. Y. Wang, "Parallel imaging: A new theoretical framework for image generation," *Pattern Recognition and Artificial Intelligence*, vol. 30, no. 7, pp. 577–587, 2017.
- [24] A. Mikołajczyk and M. Grochowski, "Data augmentation for improving deep learning in image classification problem," in *2018 International Interdisciplinary PhD Workshop (IIPhDW)*. IEEE, 2018, pp. 117–122.
- [25] Z. Zhou, J. Y. Shin, L. Zhang, S. R. Gurudu, M. B. Gotway, and J. Liang, "Fine-tuning convolutional neural networks for biomedical image analysis: Actively and incrementally," in *CVPR*, 2017, pp. 4761–4772.
- [26] D. Tuia, M. Volpi, L. Copa, M. Kanevski, and J. Munoz-Mari, "A survey of active learning algorithms for supervised remote sensing image classification," *IEEE Journal of Selected Topics in Signal Processing*, vol. 5, no. 3, pp. 606–617, 2011.
- [27] A. Rashidnasab, P. Elangovan, M. Yip, O. Diaz, D. Dance, K. Young, and K. Wells, "Simulation and assessment of realistic breast lesions using fractal growth models," *Physics in Medicine & Biology*, vol. 58, no. 16, p. 5613, 2013.
- [28] R. Saunders, E. Samei, J. Baker, and D. Delong, "Simulation of mammographic lesions," *Academic radiology*, vol. 13, no. 7, pp. 860–870, 2006.
- [29] X. Li, E. Samei, D. Delong, R. Jones, A. Gaca, C. Hollingsworth, C. Maxfield, C. Carrico, and D. Frush, "Three-dimensional simulation of lung nodules for paediatric multidetector array ct," *The British journal of radiology*, vol. 82, no. 977, pp. 401–411, 2009.
- [30] H.-o. Shin, M. Blietz, B. Frericks, S. Baus, D. Savellano, and M. Galanski, "Insertion of virtual pulmonary nodules in ct data of the chest: development of a software tool," *European radiology*, vol. 16, no. 11, pp. 2567–2574, 2006.
- [31] A. Pezeshk, B. Sahiner, R. Zeng, A. Wunderlich, W. Chen, and N. Petrick, "Seamless insertion of pulmonary nodules in chest ct images," *IEEE Transactions on Biomedical Engineering*, vol. 62, no. 12, pp. 2812–2827, 2015.
- [32] A. F. Frangi, S. A. Tsaftaris, and J. L. Prince, "Simulation and synthesis in medical imaging," *IEEE Transactions on Medical Imaging*, vol. 37, no. 3, pp. 673–679, 2018.
- [33] W. P. Segars, B. M. Tsui, J. Cai, F.-F. Yin, G. S. Fung, and E. Samei, "Application of the 4-d xcat phantoms in biomedical imaging and beyond," *IEEE transactions on medical imaging*, vol. 37, no. 3, pp. 680–692, 2018.
- [34] E. Abadi, W. P. Segars, G. M. Sturgeon, J. E. Roos, C. E. Ravin, and E. Samei, "Modeling lung architecture in the xcat series of phantoms: Physiologically based airways, arteries and veins," *IEEE transactions on medical imaging*, 2017.
- [35] A. Chatsias, T. Joyce, M. V. Giuffrida, and S. A. Tsaftaris, "Multi-modal mr synthesis via modality-invariant latent representation," *IEEE transactions on medical imaging*, vol. 37, no. 3, pp. 803–814, 2018.
- [36] C. Baur, S. Albarqouni, and N. Navab, "Melanogans: High resolution skin lesion synthesis with gans," *arXiv preprint arXiv:1804.04338*, 2018.
- [37] P. Costa, A. Galdran, M. I. Meyer, M. Niemeijer, M. Abràmoff, A. M. Mendonça, and A. Campilho, "End-to-end adversarial retinal image synthesis," *IEEE transactions on medical imaging*, vol. 37, no. 3, pp. 781–791, 2018.
- [38] A. Bentaieb and G. Hamarneh, "Adversarial stain transfer for histopathology image analysis," *IEEE transactions on medical imaging*, vol. 37, no. 3, pp. 792–802, 2018.
- [39] S. Kazemini, C. Baur, A. Kuijper, B. van Ginneken, N. Navab, S. Albarqouni, and A. Mukhopadhyay, "Gans for medical image analysis," *arXiv preprint arXiv:1809.06222*, 2018.
- [40] I. Goodfellow, J. Pouget-Abadie, M. Mirza, B. Xu, D. Warde-Farley, S. Ozair, A. Courville, and Y. Bengio, "Generative adversarial nets," in *Advances in Neural Information Processing Systems*. Curran Associates, Inc., 2014, pp. 2672–2680.
- [41] A. Odena, C. Olah, and J. Shlens, "Conditional image synthesis with auxiliary classifier gans," *arXiv preprint arXiv:1610.09585*, 2016.
- [42] A. Holzinger, M. Dehmer, and I. Jurisica, "Knowledge discovery and interactive data mining in bioinformatics-state-of-the-art, future challenges and research directions," *BMC bioinformatics*, vol. 15, no. 6, p. 11, 2014.
- [43] R. J. Gillies, P. E. Kinahan, and H. Hricak, "Radiomics: images are more than pictures, they are data," *Radiology*, vol. 278, no. 2, pp. 563–577, 2015.
- [44] P. Lambin, R. T. Leijenaar, T. M. Deist, J. Peerlings, E. E. de Jong, J. van Timmeren, S. Sanduleanu, R. T. Larue, A. J. Even, A. Jochems *et al.*, "Radiomics: the bridge between medical imaging and personalized

- medicine,” *Nature Reviews Clinical Oncology*, vol. 14, no. 12, p. 749, 2017.
- [45] R. Seising, C. Schuh, and K.-P. Adlassnig, “Medical knowledge, fuzzy sets and expert systems,” in *Workshop on intelligent and adaptive systems in medicine*, 2003.
 - [46] S. T. Kim, H. Lee, H. G. Kim, and Y. M. Ro, “Icadx: interpretable computer aided diagnosis of breast masses,” in *Medical Imaging 2018: Computer-Aided Diagnosis*, vol. 10575. International Society for Optics and Photonics, 2018, p. 1057522.
 - [47] C. J. D’Orsi, *ACR BI-RADS atlas: breast imaging reporting and data system*. American College of Radiology, 2013.
 - [48] I. C. Moreira, I. Amaral, I. Domingues, A. Cardoso, M. J. Cardoso, and J. S. Cardoso, “Inbreast: toward a full-field digital mammographic database,” *Academic radiology*, vol. 19, no. 2, pp. 236–248, 2012.
 - [49] Y. Jin, H. Wang, T. Chugh, D. Guo, and K. Miettinen, “Data-driven evolutionary optimization: An overview and case studies,” *IEEE Transactions on Evolutionary Computation*, 2018.
 - [50] P. Isola, J.-Y. Zhu, T. Zhou, and A. A. Efros, “Image-to-image translation with conditional adversarial networks,” *arXiv preprint*, 2017.
 - [51] A. Radford, L. Metz, and S. Chintala, “Unsupervised representation learning with deep convolutional generative adversarial networks,” *arXiv preprint arXiv:1511.06434*, 2015.
 - [52] V. Patel, “A framework for secure and decentralized sharing of medical imaging data via blockchain consensus,” *Health informatics journal*, p. 1460458218769699, 2018.
 - [53] S. Shubbar, “Ultrasound medical imaging systems using telemedicine and blockchain for remote monitoring of responses to neoadjuvant chemotherapy in womens breast cancer: Concept and implementation,” Ph.D. dissertation, Kent State University, 2017.
 - [54] M. Hölbl, M. Kompara, A. Kamišalić, and L. Z. Nemec, “A systematic review of the use of blockchain in healthcare,” 2018.
 - [55] X. Yue, H. Wang, D. Jin, M. Li, and W. Jiang, “Healthcare data gateways: found healthcare intelligence on blockchain with novel privacy risk control,” *Journal of medical systems*, vol. 40, no. 10, p. 218, 2016.
 - [56] F.-Y. Wang, Y. Yuan, C. Rong, and J. J. Zhang, “Parallel blockchain: An architecture for cps-based smart societies,” *IEEE Transactions on Computational Social Systems*, vol. 5, no. 2, pp. 303–310, 2018.
 - [57] Y. Yuan and F.-Y. Wang, “Blockchain and cryptocurrencies: Model, techniques, and applications,” *IEEE Transactions on Systems, Man, and Cybernetics: Systems*, vol. 48, no. 9, pp. 1421–1428, 2018.
 - [58] F.-Y. Wang and H.-m. Kim, “Implementing adaptive fuzzy logic controllers with neural networks: A design paradigm,” *Journal of Intelligent & Fuzzy Systems*, vol. 3, no. 2, pp. 165–180, 1995.
 - [59] K. Boegl, K.-P. Adlassnig, Y. Hayashi, T. E. Rothenfluh, and H. Leitich, “Knowledge acquisition in the fuzzy knowledge representation framework of a medical consultation system,” *Artificial intelligence in medicine*, vol. 30, no. 1, pp. 1–26, 2004.
 - [60] V. Kumar and S. Jain, “Alternate procedure for the diagnosis of malaria via intuitionistic fuzzy sets,” in *Nature Inspired Computing*. Springer, 2018, pp. 49–53.
 - [61] R. T. Ngan, M. Ali *et al.*, “ δ -equality of intuitionistic fuzzy sets: a new proximity measure and applications in medical diagnosis,” *Applied Intelligence*, vol. 48, no. 2, pp. 499–525, 2018.
 - [62] K. Adlassnig and G. Kolarz, “Computer-assisted medical diagnosis using fuzzy subsets,” *Approximate Reasoning in Decision Analysis (North-Holland, Amsterdam, 1982)*, pp. 219–248, 1982.
 - [63] A. Holzinger, C. Biemann, C. S. Pattichis, and D. B. Kell, “What do we need to build explainable ai systems for the medical domain?” *arXiv preprint arXiv:1712.09923*, 2017.
 - [64] X. Wang, Y. Peng, L. Lu, Z. Lu, and R. M. Summers, “Tienet: Text-image embedding network for common thorax disease classification and reporting in chest x-rays,” in *Proceedings of the IEEE Conference on Computer Vision and Pattern Recognition*, 2018, pp. 9049–9058.